Journal of Hazardous Materials 191 (2011) 1–7

Contents lists available at ScienceDirect

Journal of Hazardous Materials

journal homepage: www.elsevier.com/locate/jhazmat

Fast kinetic and efficient removal of As(V) from aqueous solution using anion exchange resins

Ahmed M. Donia, Asem A. Atia*, Dalia H. Mabrouk

Chemistry Department, Faculty of Science, Menoufia University, Shebin El-Kom, Egypt

ARTICLE INFO

Article history:
Received 17 October 2010
Accepted 12 January 2011
Available online 19 January 2011

Keywords:
Adsorption
Kinetics
Anion exchange resins
Arsenic
Water treatment

ABSTRACT

Glycidyl methacrylate/methelenebisacrylamide resin with immobilized tetraethylenepentamine ligand was prepared. This pentamine containing resin was transformed to two anion exchange resins through treatment by glycidyl trimethylammonium chloride to give (RI) or hydrochloric acid giving (RII). The resins were used to adsorb As(V) at different experimental conditions using batch and column methods. Kinetics and thermodynamic properties as well as the mechanism of interaction between As(V) and resin active sites were discussed. The maximum adsorption capacities of As(V) on RI and RII were found to be 1.83 and 1.12 mmol/g, respectively. The regeneration and the durability of the loaded resin towards the successive reuse were also investigated.

1. Introduction

Arsenic belongs to group (15) and usually is classified as a non-metal with some metallic properties. It is odorless, tasteless, and highly toxic. Inorganic arsenic can exist in four oxidation states: +5, +3, 0 and −3. The most prevalent forms in aqueous solutions are the pentavalent arsenate ion, As(V), and the trivalent arsenite ion, As(III) [1–5]. Organic forms of arsenic also exist and contribute to the total arsenic. Long and short exposure to (small/larger) amounts of arsenic causes toxicity and increased the risk to cancer [6–8]. Considering these health problems, the maximum contaminant level for arsenic in drinking water was reduced from 0.05 to 0.01 mg/L [9–11]. Several methods have been reported on the removal of arsenic, including reverse osmosis, ultrafiltration, electrodialysis, ion exchange, adsorption, and chemical precipitation. Of all these, adsorption and ion exchange are the most efficient methods. Different adsorbents such as biological materials [11–15], mineral oxides [16,17], activated carbons [2], or polymeric resins were applied. Metal-loaded resins were also successfully used. For example, iron(III)-containing resins were studied for the removal of As(III) and/or As(V) from aqueous solution [18,19]. The removal of As(V) from aqueous solutions using molybdate impregnated resin beads was also reported [20,21]. Copper(II)-loaded chelating resins with different supports were tested for the removal of As(V) [22,23]. An et al. [24] studied the selective removal of arsenate from drinking water using polystyrene supported polymeric ligand exchangers. They found that the uptake of the investigated ion exchangers is strongly affected by the solution pH which governs the speciation of arsenate. The modified coconut coir pith and lignocellulosic residue, through the successive reactions with epichlorohydrin, dimethylamine and hydrochloric acid were efficiently used for the removal of As(V) from aqueous solution and ground water [25].

In our group of research, we earlier reported on the preparation and uptake characteristics of glycidyl methacrylate/N,N′-methylenebisacrylamide (GMA/MBA) resins immobilized with tetraethylenepentamine (TEP) [26]. This pentamine containing resin was also transformed to anion exchange resin with quaternary ammonium chloride functionalities and applied for the recovery of chromate. In the present work the uptake behaviour of two anion exchange resins towards As(V) will be studied. These two anion exchangers were obtained from GMA/MBA containing tetraethylenepentamine functionality through the treatment by hydrochloric acid or glycidyl trimethylammonium chloride. The uptake characteristics have been studied using batch and column methods at different experimental conditions. Kinetics and thermodynamic parameters of the uptake process will also be calculated and discussed. The regeneration of the loaded resins for the repeated use will be investigated.

2. Experimental

2.1. Chemicals

Glycidyl methacrylate (GMA), N,N′-methylenebisacrylamide (MBA) and benzoyl peroxide (Bz_2O_2) were Aldrich products. All other chemicals were Prolabo products and were used as received. Sodium arsenate [$Na_2HAsO_4{\cdot}7H_2O$] was used as a source of As(V).

* Corresponding author. Tel.: +20 106067616; fax: +20 28356871.
E-mail address: asem_chem@yahoo.com (A.A. Atia).

0304-3894/$ – see front matter © 2011 Published by Elsevier B.V.
doi:10.1016/j.jhazmat.2011.01.056

2.2. Preparation of resins

Glycidyl methacrylate/N,N′-methylenebisacrylamide (GMA/MBA) resin was prepared through the polymerization of glycidyl methacrylate (GMA) in the presence of N,N′-methylenebisacrylamide (MBA) as a cross-linking agent at a weight ratio of 9.9:0.1, respectively. A 0.1 g Bz_2O_2 (initiator) was added to the mixture of GMA/MBA with stirring. One milliliter isopropyl alcohol and 12.6 mL cyclohexane were mixed and then added to the former solution. All the contents were then poured into a flask containing 73 mL (1%) polyvinyl alcohol and heated on a water bath at 70–80 °C with continuous stirring for 3 h. A heavy white precipitate was formed, filtered off and washed with methanol to remove the unreacted materials and then dried in air [27].

The GMA/MBA resin obtained above was loaded by tetraethylenepentamine (TEPA) as follows: one gram of the resin was added to 2 g of TEPA dissolved in 12 mL dimethyl formamide (DMF). The reaction mixture was refluxed at 75–80 °C for 72 h in an oil bath. The product obtained was filtrated off, washed with methanol and then dried in air and referred as GMA/MBA-TEPA [26].

The concentration of amino group on GMA/MBA-TEPA resin was estimated using a volumetric method [28]. A 100 mL of 0.05 M HCl solution was added to 0.5 g resin and conditioned for 15 h on a Vibromatic-384 Shaker, Gallenkamb, England. The residual concentration of HCl was estimated through the titration against 0.05 M NaOH solution and phenolphthalein as indicator using equation

$$\text{concentration of amino groups} = \frac{(M_1 - M_2) \times 100}{0.5} (\text{mmol/g resin}) \quad (1)$$

where M_1 and M_2 are the initial and final concentrations of HCl, respectively.

2.2.1. Preparation of anion exchangers

a) Four grams of GMA/MBA-TEPA resin were suspended in 50 mL of DMF/water mixture (1:1, v/v). To this mixture, 6 mL of glycidyl trimethylammonium chloride (GTA) was added and heated at 60 °C for 24 h. The product was successively washed with distilled water, methanol and acetone. The product obtained was dried in air and then referred by RI [26].
b) Four grams of GMA/MBA-TEPA resin were conditioned in 500 mL of 0.2 M HCl on a Vibromatic shaker at 300 rpm for 4 h at room temperature [25]. The conditioned resin obtained was filtered off, washed carefully with distilled water, dried at 80 °C and then referred by RII.

2.3. Adsorption measurements

2.3.1. Preparation of As(V) solution and concentration measurements

Stock solution (1×10^{-2} M) of As(V) was prepared from sodium arsenate in distilled water. The desired concentrations were then obtained by dilution. The concentration of As(V) was measured using the molybdene blue spectrophotometric method [29]. Calibration curve of As(V) in distilled water was constructed from the absorbance against concentration of As(V) at λ_{max} (870 nm). The measurements were carried out using UV/visible spectrophotometer, DR 5000, Hack. The path cell length was 1.0 cm.

2.3.2. Batch method

The adsorption of As(V) by the studied resins at different experimental conditions was carried out.

2.3.2.1. Effect of pH. A 0.1 g portion of dry resins was placed in a series of flasks each contains 100 mL of 1×10^{-3} M of As(V) solution. The desired pH of the solution was adjusted using 0.1 N HCl and 1 N NaOH. The flasks were conditioned on a Vibromatic shaker at 300 rpm for 1 h at 25 °C. The uptake of As(V) was calculated by determining the residual concentration of As(V) following the above method and according to equation

$$q_e = \frac{(C_o - C_e) \times 100}{0.1} (\text{mmol/g resin}) \quad (2)$$

where q_e is the uptake of As(V) at equilibrium, C_o and C_e are the initial and equilibrium concentrations of As(V), respectively.

2.3.2.2. Effect of time. A 0.1 g portion of dry resin was placed in flasks containing 100 mL of 1×10^{-3} M of As(V) at pH 6 for RI and pH 4.6 for RII. The contents of the flasks were equilibrated on the shaker at 300 rpm and 25 °C. Ten mL of the solution (free from resins particles) were taken from the flasks at different time intervals and the residual concentration of As(V) was determined.

2.3.2.3. Adsorption isotherms. The effect of initial concentration of As(V) on the adsorption was carried out by placing 0.1 g portions of dry resin in a series of flasks each containing 100 mL of As(V) with different concentrations at pH 6 for RI and pH 4.6 for RII. The contents of the flasks were equilibrated on the shaker at 300 rpm and at 25, 33, 40 and 50 °C for 15 min. After equilibration, the residual concentration of As(V) in each flask was determined to calculate the amount adsorbed of As(V).

2.3.3. Column method

Flow experiments were performed in a plastic column (length 5 cm, diameter 1 cm). A small piece of glass wool was placed at the bottom of the column and then a known quantity of the resins under investigation was placed in the column (bed height 2 cm). A solution of As(V) with initial concentration of 5×10^{-4} M was allowed to flow downward through the column with different flow rates. The concentration of As(V) in the outlet was analyzed at different time intervals. The experiment was terminated when the concentration of the As(V) at the outlet of the column equals its initial concentration. The effect of bed height was also studied using 1–3 cm bed height at flow rate of 1 mL/min.

2.4. Regeneration of the loaded resin

Regeneration experiments were performed by placing 0.5 g of resins in the column then loaded with As(V) at flow rate 1 mL/min. After reaching the maximum uptake, the resin was washed carefully by flowing distilled water through the column. The resin loaded by As(V) was then subjected for regeneration using 1 M HCl. The resin was then carefully washed with distilled water to become ready for the second run of loading with As(V). The regeneration efficiency was calculated according to equation

$$\text{regeneration efficiency (\%)} = \frac{\text{uptake in the 2nd run}}{\text{uptake in the 1st run}} \times 100 \quad (3)$$

3. Results and discussions

3.1. Preparation of the resins

The structures of the prepared resins are given in Scheme 1 [26].

3.2. Batch method

3.2.1. Effect of pH

Generally, and as shown in Fig. 1, the As(V) uptake of the two resins against the pH changes is mainly the same, except the slight

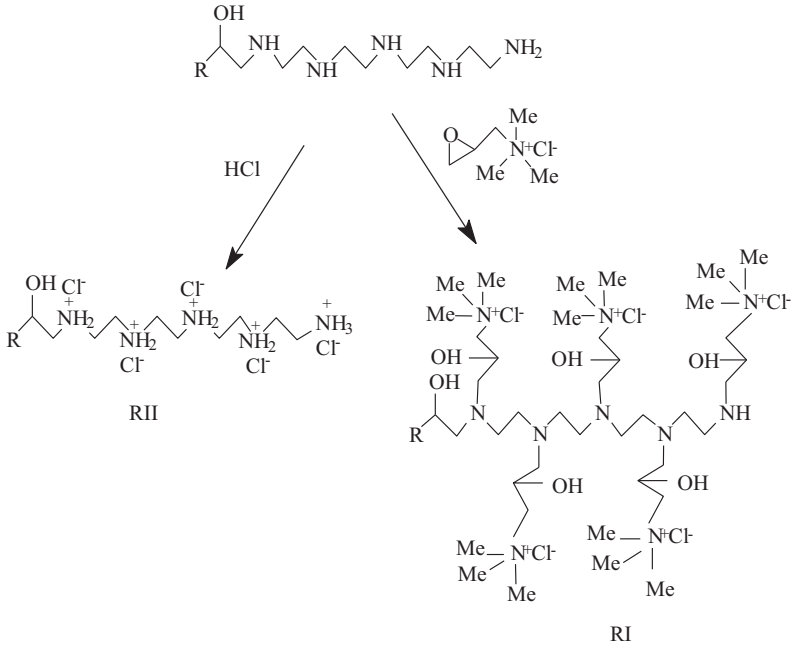

Scheme 1. Preparation of resins RI and RII.

shift in pH of maximum uptake (about 1 unit). This shift may be related to the structural change of the resins (Scheme 1). The uptake/pH behaviour of both resins towards As(V) can be interpreted on the basis of arsenate speciation [24,25] as follows:(i) at pH lower than 2, the predominant arsenate species is the uncharged form ($H_3AsO_4{}^0$) which display no interaction with the positively charged active sites; (ii) above pH 2–7, as the pH increase the concentration of dihydrogen monobasic form ($H_2AsO_4{}^-$) increases which successfully interact with positive surface of the resins giving higher uptake; (iii) above pH 7, the monohydrogen dibasic form ($HAsO_4{}^{2-}$) starts in formation and its concentration increases with the pH. In spite of the efficient interaction of $HAsO_4{}^{2-}$ (more than $H_2AsO_4{}^-$) with the positive surface of the resins, it is competed with the higher concentration of OH^- giving a dramatic lower uptake.

3.2.2. Kinetics

The adsorption of As(V) by RI and RII as a function of time is shown in Fig. 2. Clearly, the equilibrium was reached after 5 min in both resins. This fast rate of adsorption makes these resins promising for practical applications in comparison with other reported ones. The equilibrium time of some previously studied resins extends from 2 h up to few days [19–21]. The data obtained in Fig. 2 was treated according to pseudo-second order kinetics model [30]

$$\frac{t}{q_t} = \frac{1}{k_2 q_e^2} + \left(\frac{1}{q_e}\right) t \quad (4)$$

where q_e and q_t refer to the amount of As(V) adsorbed at equilibrium and at time t, respectively (mmol/g), and k_2 is the overall rate constant of the pseudo-second order adsorption (g/mmol min). The linear plots of t/q_t versus t of the adsorption data of As(V) on the resins are shown in Fig. 3. The pseudo-second order rate constant k_2 and equilibrium adsorption capacity q_e, were calculated from the values of intercepts and slopes, respectively and reported in Table 1. The values of calculated q_e are in good agreement with the experimental ones. This implies that the adsorption processes follows pseudo-second order kinetics. The values of rate constant for RII > RI. This may be attributed to the steric effect exerted by the methyl group substituents on positive nitrogen active site.

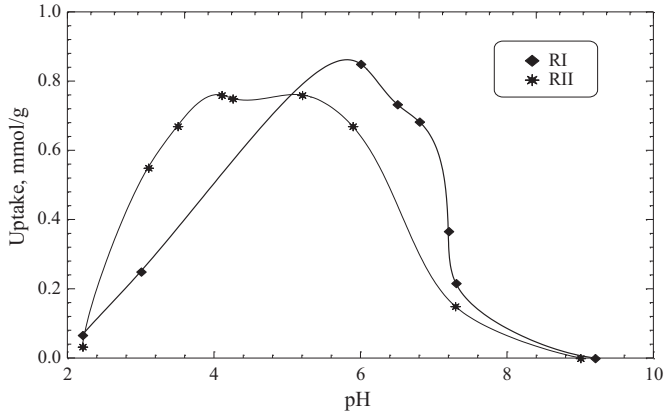

Fig. 1. Effect of pH on the adsorption of As(V) by RI and RII at concentration of 1×10^{-3} M, 1 h equilibrium time and 25 °C.

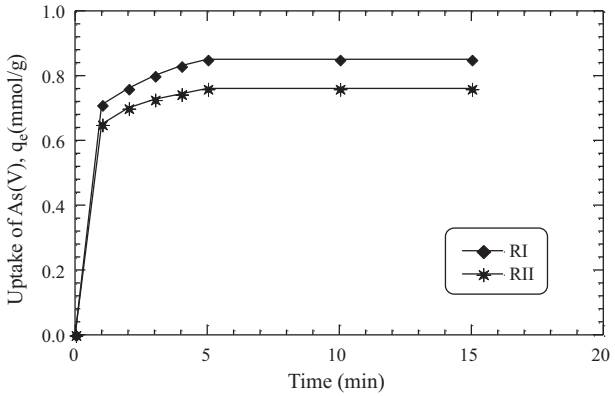

Fig. 2. Effect of time on the adsorption of As(V) by RI and RII at initial concentration of 1×10^{-3} and 25 °C.

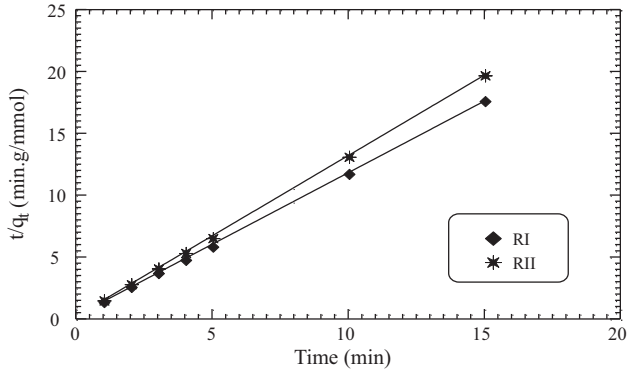

Fig. 3. Pseudo-second order plots of the adsorption of As(V) on RI and RII.

Table 1
Pseudo-second order kinetic data for adsorption of As(V) on resins at 25 °C.

Resin	$q_e^{(exp.)}$ (mmol/g)	$q_e^{(calc.)}$ (mmol/g)	k_2 (g/mmol min)	R^2
RI	0.85	0.86	5.8	0.9998
RII	0.76	0.77	8.28	0.9999

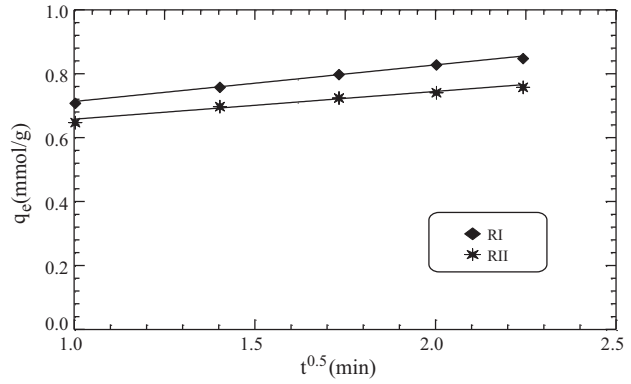

Fig. 4. Intraparticle diffusion plot of the adsorption of As(V) on RI and RII.

To examine the rate determining step of the adsorption reaction, the uptake time data obtained were treated according to the equation [31]

$$q_t = x + k_i t^{0.5} \quad (5)$$

where k_i (mmol/g min$^{0.5}$) is the intraparticle diffusion rate constant and x is indication for the thickness of the boundary layer. The straight line obtained and the positive values of x (Fig. 4 and Table 2) indicate that the adsorption rate of the two resins is controlled by the intraparticle diffusion and the boundary layer. The higher value of x for RI can be related to the steric as well as the hydrophobic effect of methyl group.

3.2.3. Adsorption isotherms

Adsorption isotherm data at different temperatures (Fig. 5) were treated according to Langmuir model

$$\frac{C_e}{q_e} = \frac{C_e}{Q_{max}} + \frac{1}{K_L Q_{max}} \quad (6)$$

Table 2
The intraparticle diffusion data for adsorption of As(V) on resins at 25 °C.

Resin	k_i (mmol/g min$^{0.5}$)	x	R^2
RI	0.1144	0.6	0.996
RII	0.0868	0.57	0.98

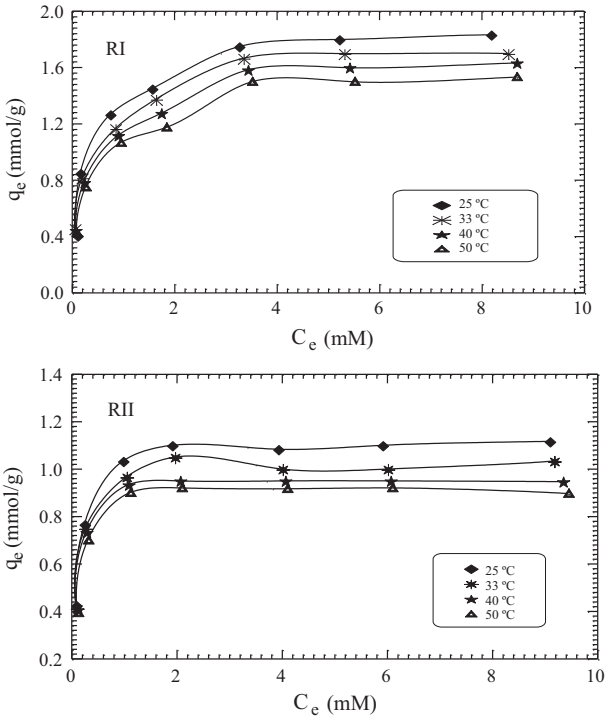

Fig. 5. Adsorption isotherms of As(V) on RI and RII at different temperatures.

where C_e is the equilibrium concentration of As(V) in solution (mmol/L), q_e is the amount adsorbed at C_e (mmol/g), Q_{max} is the maximum adsorption capacity (mmol/g), and K_L is the binding constant of Langmuir which is related to the energy of adsorption (L/mmol). Plotting C_e/q_e against C_e gives straight line with slope and intercept equal to $1/Q_{max}$ and $1/K_L Q_{max}$, respectively (Fig. 6). The values of K_L and Q_{max} at different temperatures are reported in Table 3. The values of Q_{max} obtained at different temperatures are in good agreement with the experimental ones. This indicates that the adsorption is a monolayer and proceeds according to Langmuir model. Inspection of the changes in K_L values with temperature (Table 3) indicates that the two resins display two different behaviours. This can be explained on the basis of different structural features of the two resins (Scheme 1) as follows: (i) RI is more hydrophobic (less hydrophilic) than RII due to the presence of methyl group substituents on positive nitrogen active sites; (ii) as the temperature increases the vibrational motion of the methyl groups of RI increases which subsequently increases their steric effects. These steric effects decrease the interaction between arsenate anion and active site giving lower K_L values; (iii) the observed different behaviours in K_L values of RII with temperature increase may be related to the presence of hydrophilic ($-N^+H_2/-N^+H_3$) moieties (with no hydrophobic steric substituent $-CH_3$). As the temperature increases the dehydration of active sites ($-N^+H_2/-N^+H_3$) increases giving a strong arsenate interaction (higher K_L values); (iv) the lower K_L values of RI relative to those of RII may be related to the steric and electronic effects of methyl

Table 3
Langmuir parameters for adsorption of As(V) on resins at different temperatures.

Temp. (°C)	$q_e^{(exp.)}$ (mmol/g)		Q_{max} (mmol/g)		K_L (L/mmol)	
	RI	RII	RI	RII	RI	RII
25 °C	1.83	1.12	1.88	1.13	3.93	09.551
33 °C	1.70	1.03	1.76	1.04	3.66	0.791
40 °C	1.63	0.95	1.69	0.96	3.11	6.892
50 °C	1.53	0.90	1.59	0.91	2.66	4.61

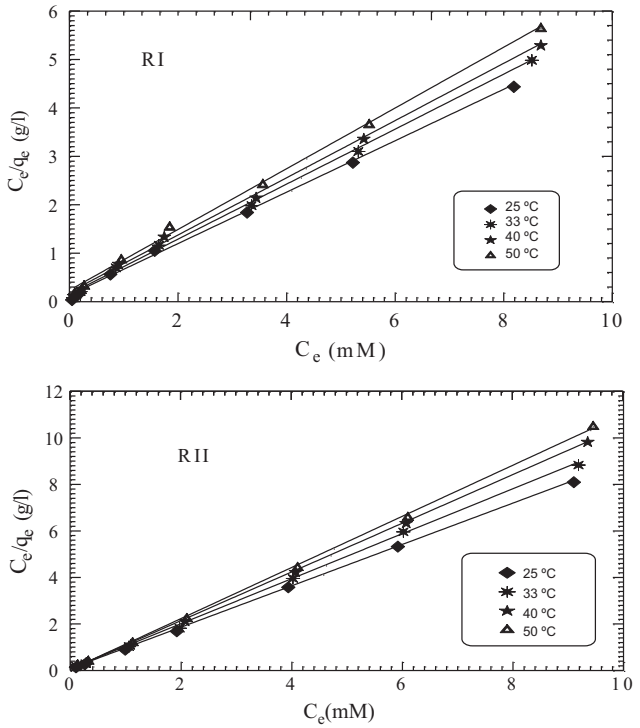

Fig. 6. Langmuir adsorption plots of As(V) by RI and RII at different temperatures.

group substituent on positive nitrogen active sites. These effects hinder the interaction of arsenate anion by steric hindrance and lowering the positive charge on nitrogen by hyper conjugation of methyl group.

The essential features of Langmuir adsorption isotherm can be expressed in terms of a dimensionless constant called separation factor (R_L) which is defined by the following equation [32]

$$R_L = \frac{1}{1 + K_L C_o} \tag{7}$$

where C_o is the initial concentration of the metal ion (mmol/L). The values of R_L indicate the nature of the adsorption to be irreversible ($R_L = 0$), favorable ($0 < R_L < 1$) and unfavorable ($R_L = 1$). The values of R_L obtained according to the above equation are 0.202 and 0.025 for RI but RII gives 0.095 and 0.010 at initial As(V) concentration of 1×10^{-3} M and 1×10^{-2} M, respectively. This implies that the adsorption of As(V) on both RI and RII from aqueous solution is favorable under the conditions used in this study. The thermodynamic parameters of the adsorption reaction were calculated using van't Hoff equation [33]

$$\ln K_L = \frac{-\Delta H^\circ}{RT} + \frac{\Delta S^\circ}{R} \tag{8}$$

where K_L is Langmuir binding constant (L/mmol), R is the universal gas constant (8.314 J/mol K), T is the absolute temperature (Kelvin). Plotting of $\ln K_L$ against $1/T$ gives straight lines with slope and intercepts equal $-\Delta H^\circ/R$ and $\Delta S^\circ/R$, respectively (Fig. 7). The negative values of both ΔH° and ΔS° for RI (Table 4) indicate an exothermic adsorption reaction accompanied with more ordered state [33]. While the positive values of both ΔH° and ΔS° for RII indicate an endothermic adsorption process with more randomness due to the liberation of water molecules. The Gibbs free energy ΔG° of the adsorption reactions were also obtained using the following relation and given in Table 4.

$$\Delta G^\circ = \Delta H^\circ - T\Delta S^\circ \tag{9}$$

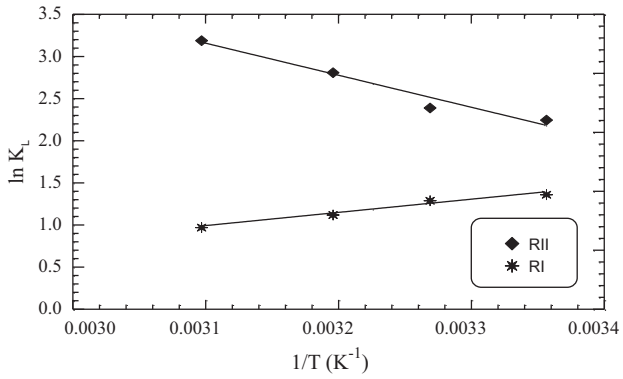

Fig. 7. Van't Hoff plots for the adsorption of As(V) on RI and RII.

The negative values of ΔG° indicate that the adsorption is spontaneous. For RI, ΔG° decrease as temperature increase which indicates that the process of adsorption of As(V) becomes less favorable at higher temperatures. This may be again attributed to the increased steric effect of the methyl groups due to their increased vibrational motion with temperature. For RII as temperature increases the reaction becomes more favorable due to the liberation of water molecules from the active sites. On the other hand, the data given in Table 4 for RI shows that $|T\Delta S^\circ| < |\Delta H^\circ|$ at all temperatures. This indicates that the adsorption reaction is dominated by enthalpic rather than entropic changes. But for RII the adsorption reaction is dominated by entropic rather than enthalpic where $|T\Delta S^\circ| > |\Delta H^\circ|$ at all temperatures. These thermodynamic features of the resins towards the adsorption of arsenate confirm our suggestion on the effective role of the structural characteristics of the resins on the strength of interaction.

3.3. Column studies

3.3.1. Effect of flow rate

The breakthrough curves of the resins towards As(V) at different flow rates (1–3 mL/min) and a fixed bed height of 2 cm are shown in Fig. 8. The breakthrough points of RII occurred faster than that of RI at all flow rates and the breakthrough curves become sharper as flow rate increases. This behaviour may be attributed to the higher capacity of the resin RI towards As(V) anions rather than RII and makes it promising in the field of water and wastewater treatment.

3.3.2. Effect of bed height

The effect of bed height of RI and RII was studied at 1–3 cm while the flow rate was held constant at 1 mL/min. The data obtained are shown in Fig. 9. The influence of bed heights was tested in terms of breakthrough time (t_b) and saturation time (t_s). The uptake values of the resins were found to be directly proportional with bed height. Bed depth service time model (BDST) is a simple model that relates between bed height (Z) and saturation time (t_s) of the column through the following equation [34]

$$t_s = \frac{N_o Z}{C_o \nu} - \frac{1}{K_a C_o} \ln\left(\frac{C_o}{C_t} - 1\right) \tag{10}$$

where C_t (mmol/L) is the concentration of As(V) at the saturation time (i.e. $C_o/C_t = 100/99$), C_o (mmol/L) the initial concentration, N_o is the total adsorption capacity (mmol of adsorbate/L of adsorbent), ν the linear velocity (cm/min) and K_a is the rate constant of adsorption (L/mmol min). The values of N_o and K_a were calculated from the slopes and intercepts of the BDST plots. The calculated values of N_o were found to be comparable with the experimental values of q_s. This indicates the validity of the BDST model for the investigated resins. If K_a is large, even a short resin bed will avoid the

Table 4
Thermodynamic parameters for adsorption of As(V) on the resins.

Temp. (K)	ΔH° (kJ/mol)		ΔS° (kJ/mol K)		ΔG° (kJ/mol)		$\lvert T\Delta S^\circ\rvert$ (kJ/mol)	
	RI	RII	RI	RII	RI	RII	RI	RII
298	−13.03	+31.6	−0.03	0.124	−3.45	−5.35	9.57	36.95
306					−3.20	−6.34	9.83	37.94
313					−2.97	−7.21	10.05	38.81
323					−2.65	−8.45	10.38	40.05

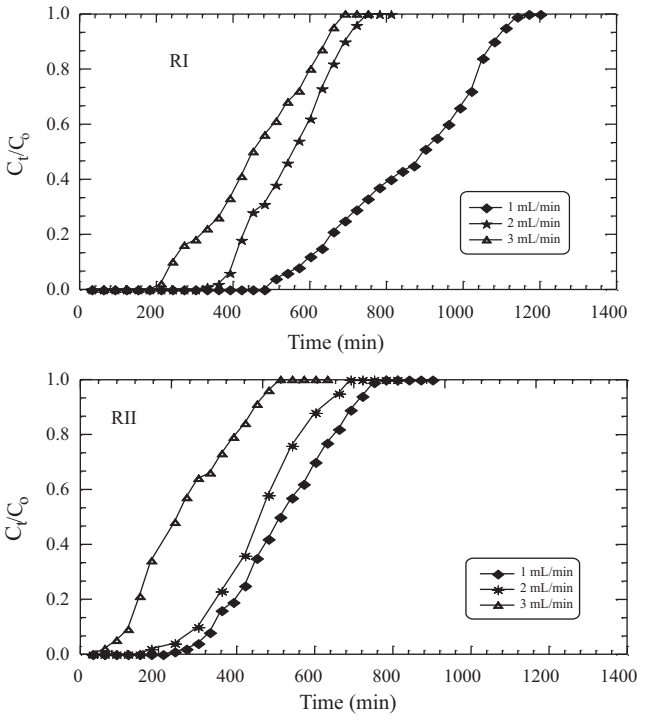

Fig. 8. The breakthrough curves of RI and RII towards As(V) at different flow rates and a bed height of 2 cm.

breakthrough limit. In case of small values of K_a a progressively longer bed would be required to delay the breakthrough point. The values of K_a for resins are 0.057 and 0.032 (L/mmol min) for RI and RII, respectively. The critical bed height (Z_o) can be calculated by setting $t_s = 0$ in Eq. (6) and rearranging to get

$$Z_o = \frac{v}{K_a N_o} \ln\left(\frac{C_o}{C_b} - 1\right) \quad (11)$$

where C_b is the breakthrough metal ion concentration (mmol/L). The above equation implies that Z_o depends on the kinetics of the sorption process, the residence time of the solute and the adsorption capacity of the resins. Thus the critical bed height of the resin was recorded as 0.29 and 1.3 cm for RI and RII, respectively. This indicates the higher efficiency of the resins for the removal of As(V).

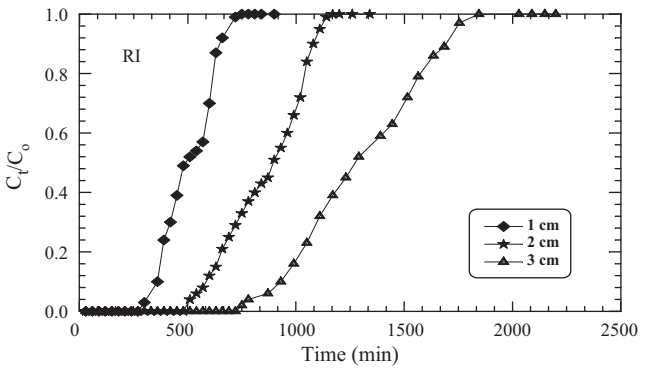

Fig. 9. The effect of bed heights of RI and RII on the adsorption of As(V) at a flow rates of 1 mL/min.

3.4. Regeneration

For cost reduction purposes, regeneration of the resin was done using 1 M HCl. Adsorption/desorption of the charged column with the resins was carried out for several times. Regeneration efficiency was found to be 99% and 98% for RI and RII, respectively.

4. Conclusion

The anion exchangers obtained are characterized by fast and higher adsorption capacities towards As(V) from aqueous media at pH (4–7). The equilibrium adsorption was reached within 5 min for both resins. The adsorption process was found to follow pseudo-second order kinetics. The difference in thermodynamic behaviour of two exchangers was affected by methyl group substituent on positive nitrogen active sites. Column studies give an account about the breakthrough points at different flow rates and bed heights. The critical bed height of the resin towards As(V) was found to be 0.29 and 1.3 cm, respectively. The regeneration efficiency of the loaded resins was found to be 99 and 98% for RI and RII, respectively using 1 M HCl. The data obtained indicate that the studied resins are promising for As(V) removal relative to the early reported ones [19–21].

References

[1] S.Y. Thomas, T.G. Choong, Y. Chuah, F.L. Robiah, Koay Gregory, I. Azni, Arsenic toxicity, health hazards and removal techniques from water: an overview, Desalination 217 (2007) 139–166.
[2] L. Lorenzen, J.S.J. van Deventer, W.M. Landi, Factors affecting the mechanism of the adsorption of arsenic species on activated carbon, Miner. Eng. 8 (4/5) (1995) 557–569.
[3] D. Mohan, C.U. Pittman, Arsenic removal from water/wastewater using adsorbents: a critical review, J. Hazard. Mater. 142 (2007) 1–5.
[4] E.O. Kartinen Jr., C.J. Martin, An overview of arsenic removal processes, Desalination 103 (1995) 79–88.
[5] T.S. Singh, K.K. Pant, Equilibrium, kinetics and thermodynamic studies for adsorption of As(III) on activated alumina, Sep. Purif. Technol. 36 (2004) 139–147.
[6] M.J. DeMarco, A.K. Sengupta, J.E. Greenleaf, Arsenic removal using a polymeric/inorganic hybrid sorbent, Water Res. 37 (2003) 164–176.
[7] J.T. Mayo, C. Yavuz, S. Yean, L. Cong, H. Shipley, W. Yu, J. Falkner, A. Kan, M. Tomson, V.L. Colvin, The effect of nanocrystalline magnetite size on arsenic removal, Sci. Technol. Adv. Mater. 8 (2007) 71–75.
[8] S. Bang, G.P. Korfiatis, X. Meng, Removal of arsenic from water by zero-valent iron, J. Hazard. Mater. 121 (2005) 61–67.
[9] A.E. Pagana, S.D. Sklari, E.S. Kikkinides, V.T. Zaspalis, Microporous ceramic membrane technology for the removal of arsenic and chromium ions from contaminated water, Micropor. Mesopor. Mater. 110 (2008) 150–156.
[10] V. Zaspalis, A. Pagana, S. Sklari, Arsenic removal from contaminated water by iron oxide sorbents and porous ceramic membranes, Desalination 217 (2007) 167–180.
[11] S. Kundu, A.K. Gupta, Adsorption characteristics of As(III) from aqueous solution on iron oxide coated cement (IOCC), J. Hazard. Mater. 142 (2007) 97–104.
[12] R. Devi, E. Alemayehu, V. Singh, A. Kumar, E. Mengistie, Removal of fluoride, arsenic and coliform bacteria by modified homemade filter media from drinking water, Biores. Technol. 99 (2008) 2269–2274.
[13] T. Halttunen, M. Finell, S. Salminen, Arsenic removal by native and chemically modified lactic acid bacteria, Int. J. Food Microbiol. 120 (2007) 173–178.

[14] A. Oehmen, R. Viegas, S. Velizarov, M.A.M. Reis, J.G. Crespo, Removal of heavy metals from drinking water supplies through the ion exchange membrane bioreactor, Desalination 199 (2006) 405–407.
[15] P. Mondal, C.B. Majumder, B. Mohanty, Treatment of arsenic contaminated water in a laboratory scale up-flow bio-column reactor, J. Hazard. Mater. 153 (2008) 136–145.
[16] H. Sun, L. Wang, R. Zhang, J. Sui, G. Xu, Treatment of groundwater polluted by arsenic compounds by zero valent iron, J. Hazard Mater. B 129 (2006) 297–303.
[17] L. Cumbal, J. Greenleaf, D. Leun, A.K. Sengupta, Polymer supported inorganic nanoparticles: characterization and environmental applications, React. Funct. Polym. 54 (2003) 167–180.
[18] M.J. Haron, W.M.Z. Wan Yunus, N.L. Yong, S. Tokunaga, Sorption of arsenate and arsenite anions by Iron(III)–poly(hydroxamic acid) complex, Chemosphere 39 (14) (1999) 2459–2466.
[19] H. Matsunga, T. Yokoyama, R.J. Eldridge, B.A. Bolto, Adsorption characteristic of arsenic(III) and arsenic(V) on iron(III)-loaded chelating resin having lysine-N,N-diacetic acid moiety, React. Funct. Polym. 29 (1996) 167–174.
[20] L. Dambies, E. Guibal, A. Roze, Arsenic(V) sorption on molybdate-impregnated chitosan beads, Colloids Surf. A: Physicochem. Eng. Aspects 170 (2000) 19–31.
[21] T. Balaji, T. Yokoyama, H. Matsunaga, Adsorption and removal of As(V) and As(III) using Zr-loaded lysine diacetic acid chelating resin, Chemosphere 59 (2005) 1169–1174.
[22] G.E. Fryxell, J. Liu, T.A. Hauser, Z. Nie, K.F. Ferris, S. Mattigod, M. Gong, R.T. Hallen, Design and synthesis of selective mesoporous anion traps, Chem. Mater. 11 (1999) 2148–2154.
[23] A. Ramana, A.K. Sengupta, Removing selenium(IV) and Arsenic(V) oxyanions with tailored chelating polymers, J. Environ. Eng. 118 (5) (1992) 755–775.
[24] B. An, T.R. Steinwinder, D. Zhao, Selective removal of arsenate from drinking water using a polymeric ligand exchanger, Water Res. 39 (2005) 4993–5004.
[25] T.S. Anirudhan, M.R. Unnithan, Arsenic(V) removal from aqueous solutions using an anion exchanger derived from coconut Coir pith and its recovery, Chemosphere 66 (2007) 60–66.
[26] A.A. Atia, Synthesis of a quaternary amine anion exchange resin and study its adsorption behaviour for chromate oxyanions, J. Hazard. Mater. B 137 (2006) 1049–1055.
[27] A.M. Donia, A.A. Atia, H. El-Boraey, D.H. Mabrouk, Uptake studies of copper(II) on glycidyl methacrylate chelating resin containing Fe_2O_3 particles, Sep. Purif. Technol. 49 (2006) 64–70.
[28] A.A. Atia, A.M. Donia, S.A. Abou-Ei-Enein, A.M. Yousif, Studies on uptake behaviour of copper(II) and lead(II) by amine chelating resins with different textural properties, Sep. Purif. Technol. 33 (2003) 295–301.
[29] V. Lenoble, V. Deluchat, B. Serpaud, J.C. Bollinger, Arsenite oxidation and arsenate determination by the molybdene blue method, Talanta 61 (2003) 267–276.
[30] P.K. Malik, Day removal from wastewater using activated carbon developed from sawdust: adsorption equilibrium and kinetics, J. Hazard. Mater. 113 (2004) 81–88.
[31] L. Karim, S. Nacer, G. Bilango, Kinetics of chromiumsorption on biomass fungi from aqueous solution, Am. J. Environ. Sci. 2 (1) (2006) 31–36.
[32] A.A. Atia, Adsorption of chromate and molybdate by cetylpyridinium bentonite, Appl. Clay Sci. 41 (2008) 73–84.
[33] F. Gode, E. Pehlivan, A comparative study of two chelating ion-exchange resins for the removal of chromium(III) from aqueous solution, J. Hazard. Mater. B 100 (2003) 231–243.
[34] K. Vijayaraghavan, J. Jegan, K. Palanivelu, M. Velan, Biosorption of cobalt(II) and nickel(II) by seaweeds: batch and column studies, Sep. Purif. Technol. 44 (1) (2005) 53–59.